Polarization analysis of CuXX-lines emitted from X-pinch

E O Baronova, Jean Larour, F B Rosmej, F y Khattak

Polarization analysis of CuXX-lines emitted from X-pinch

E O Baronova[1]**, J Larour**[2]**, F B Rosmej**[3,4]** and F Y Khattak**[5]

[1] National Research Center "Kurchatov Institute", Kurchatov Square 1, Moscow 123182, Russia

[2] Laboratoire de Physique des Plasmas, École Polytechnique, CNRS, Route de Saclay, Palaiseau F-91128, France

[3] Sorbonne Universités, Pierre et Marie Curie, UMR7605, case128, Paris Cedex 05 F-75252, France

[4] Laboratoire pour l'Utilisation des Lasers Intenses, CNRS-CEA, École Polytechnique, Physique Atomique dans les Plasmas Denses, Route de Saclay, Palaiseau F-91128, France

[5] Kohat University of Science and Technology, Department of Physics, Kohat, Khyber Pakhtunkhwa 26000, Pakistan

E-mail: `baronova04@mail.ru`

Abstract. Soft x-ray emission from CuXX L-shell lines emitted by a dense X-pinch plasma have been investigated with high-resolution curved Bragg crystals at different angles of orientation. Single shot time integrated spectra show clear evidences of polarization for the Ne-like spectral lines $2s^2 2p^6 \ ^1S_0 \rightarrow 2s^2 2p^5 3s \ ^1P_1$ ($\lambda = 12.570$ Å), $2s^2 2p^6 \ ^1S_0 \rightarrow 2s^2 2p^5 3s \ ^3P_1$ ($\lambda = 12.8277$ Å). The variation of the intensity ratio of these two well-separated L-shell lines is discussed in view of its application for suprathermal electron characterization under real experimental conditions of pinch plasmas. We demonstrated that the simultaneous use of two different polarization spectrometers (means 4 Bragg crystals) permitted a high level of confidence for the analysis of the variation of the line ratios due to polarization.

1. Introduction

Pulsed dense plasmas created in pinch discharges (plasma focus, gas puff, X-pinch, vacuum spark, capillary as well as various types of wire arrays) have attracted world-wide interest due to the large variety of plasma parameters: plasma size of the so-called hot spots (compressed dense plasma regions) of about $(10^{-4}–10^{-1})$ cm, life time less than $(1–50)$ ns, electron temperature kT_e in the range of $(0.1–10)$ keV, electron density n_e of about $(10^{18}–10^{23})$ cm^{-3}, discharge current I_{beam} rise of some 10 kA in a few ns, energy of suprathermal electrons up to 500 keV, predicted electric fields of the order of 10^{10} V/cm, energy of hard x-rays up to 300–500 keV, energy of fast ions up to few MeV [1–5]. These plasma parameters are of great interest for science and applications: high energy density physics, inertial fusion, atomic physics and spectroscopy, x-ray source, lithography, biomedical applications.

The complexity of the plasma evolution accompanied by the generation of electron beams and fast ions, the presence of hard x-rays, directed as well as turbulent electromagnetic fields challenge theory and likewise instrumentation and diagnostics. X-ray spectroscopy turns out to be one of the unique approaches to investigate such complex plasma phenomena. The determination of main plasma parameters (density, temperature) is often based on the analysis

of relative intensities of x-ray lines supposing that the electron energy distribution function is Maxwellian [5–7]. Theoretical analysis has shown an important influence of suprathermal electrons on the line intensities emitted from K- and L-shells [8–10], that in turn can be employed to characterize the electron beam parameters. One of the methods to characterize suprathermal electrons is x-ray polarization spectroscopy [9, 11]. Polarized x-ray line emission from He-like ions have been observed in solar flares [12], laser produced plasmas [13], vacuum sparks [14, 15], in plasma focus machines [16, 17], ion traps [18] and in astrophysical experiments. At present the quantitative interpretation of the observed polarization phenomena is in encouraging agreement with the data although radiative decay including the hyperfine interaction, plasma opacity, time-dependent behavior of plasma parameters are still awaiting more detailed analysis.

The present paper is devoted to the study of x-ray line polarization for the complex L-shell line emission spectra of Cu emitted from a dense X-pinch. The L-shell emission of mid-Z metals that has attracted attention in numerous laboratories [19, 20] to extract electron temperature T_e and electron density n_e from line intensity ratios. Detailed polarization analysis [21–23], however, is much less developed.

2. The origin of line polarization

Two effects give rise to polarized x-rays. The first is anisotropy of the electron velocity distribution function: collisional excitation is therefore selective in m-quantum numbers giving rise to polarized photon emission if randomizing collisions are much less frequent than radiative decay. For highly charged ions, such situation can excist even for dense plasmas because the critical density scales with the 7th power of the effective charge Z_{eff} of the ion [10]. The second effect is due to the presence of macroscopic electric fields.

If polarized x-rays are excited by an anisotropic electron velocity distribution function, the polarization from electron impact decreases in most cases monotonically with increasing energy. The degree and direction of polarization depends on the type of the transition [9, 21–23]. There are various types of plasma electrons in Z-pinches: a) beam electrons with energies comparable or even higher than the applied voltage (typical energy 10–100 keV) that are moving directly towards the anode (their runaway mechanism is discussed in [2,5]), b) the low energy part (a few keV) of runaway electrons, that redistribute themselves according to the plasma electromagnetic fields, c) the Maxwellian tail of isotropic electrons in the plasma bulk, d) current carrying thermal electrons, their velocity distribution function is a shifted Maxwellian or a slightly anisotropic version thereof.

Theoretical studies have shown that even a few percent of hot isotropic electrons in a Maxwellian tail may affect the line intensities considerably [10]. As far as concerns energetic anisotropic electrons and electron beams—they are at the origin of x-ray line polarization and corresponding polarization measurements might provide detailed information (note, that the main contribution to polarization is from electrons with the energies close to the excitation threshold).

The spatial structure of type of Z-pinch plasmas (hot spots, micro-pinches) is well known and it has been observed that x-rays originate essentially the hot spots. However, plasma size, the spatial extent of the electron beam, its duration and the interaction of the spatially anisotropic hot electrons with the multi-charged ions in the hot spot are not well known. The experimental data of polarization of x-ray lines proved, that highly ionized ions coexist with fast electrons in the same plasma volume during some time. In [24] it is supposed that the electron beam (and also the generation of electrons with a few keV) is created at the time of plasma channel breakdown and originates from the hot spot region. In these models the electron beam has an energy distribution from few keV up to few hundreds of keV, and the motion of low energy (a few keV) electrons emanating from the beam is determined by electromagnetic fields that exist inside the plasma.

The Interpretation of the polarization measurement in terms of an anisotropic electron distribution function assumes that the electron electric field dominate over the orientation of the ion during the time needed to radiate polarized x-rays [9]. Another possibility is that the plasma electric field dominates the orientation of the orbit in the excited ion [25]. In this case polarization measurements to not determine the anisotropic electron distribution, but the electric field in the plasma. The results of both models are identical when the direction of the electron velocity coincides with the electric field direction. In any case the polarization is associated with information about macroscopic fields, existing in the vicinity to an ion at the instant of photon emission resulting in line polarization.

3. Polarization technique for x-rays

According to Bragg's law x-rays are reflected by the parallel atomic planes according $2d \sin \theta_B = k\lambda$, where d is the lattice spacing, k the reflection order and λ the incident wavelength. The integrated reflectivity P_D for Bragg reflection from an ideal crystal is $P_D = AF_{hkl}\mathrm{tg}\theta_B K$, where A is the combination of the electron charge, mass and the volume of a unit cell, F_{hkl} is the structure factor for the hkl reflection. K is the polarization factor $(1 + |\cos 2\theta_B|)/2$: $K = \frac{1}{2}$ for the σ-component and $K = |\cos 2\theta_B|/2$ for the π-component. Here the σ-component has the electric field vector in the direction perpendicular to the dispersion plane and the π-component parallel to the plane. These values are for an ideal crystal, and if the crystal is ideally mosaic, the above $|\cos 2\theta_B|$ is replaced by $\cos^2 2\theta_B$.
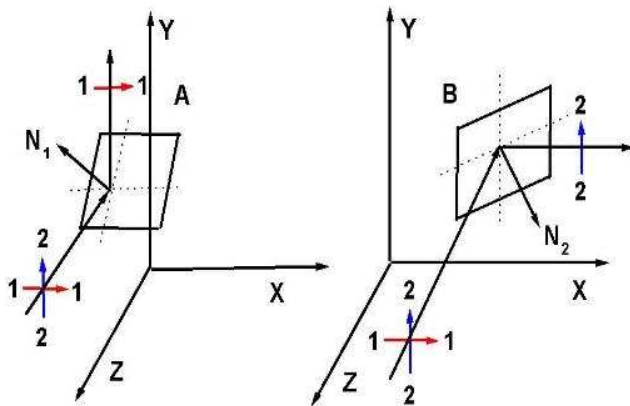

Figure 1. Schematic geometry of polarization measurements with two mutually perpendicular crystals, both at Bragg angle 45°.

At the Bragg angle of 45° the polarization separation efficiency is 1 (highest). In the close vicinity of 45° the efficiency of separation of π and σ-components depends on the type of crystal polarizer. Ideal mosaic crystals (mica, LiF, etc) are effective as they can be employed in a relatively wide range of Bragg angles: 38–52°. Contrary ideal crystals (quartz, Si, etc) serve only within a rather narrow spectral range: 44–46°.

To analyze polarization of soft x-ray emission we used two identical mica-polarizers with mutually perpendicular dispersion planes. The geometrical scheme is shown in figure1. The polarizer at the left hand side (A) reflects radiation with an electric field vector along the x axis (arrow 1-1), the spectrometer at the right hand side (B) reflects radiation with an electric field vector along the y axis (arrow 2-2).

Polarization measurements of a point like x-ray source are more easier to interpret that those for extended sources [10] and in the sections below be describe polarization spectroscopic studies of line emission originating from the hot spots. Particular attention has been devoted to the transitions in Ne-like copper (CuXX) that are proposed for plasma diagnostics [19]: $2s^2 2p^6$ $^1S_0 \rightarrow 2s^2 2p^5 3s \; ^1P_1$ at $\lambda = 12.570$ Å and $2s^2 2p^6 \; ^1S_0 \rightarrow 2s^2 2p^5 3s \; ^3P_1$ at $\lambda = 12.8277$ Å.
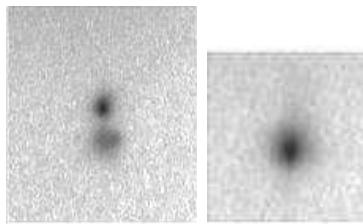
Figure 2. X-ray pinhole images demonstrating the appearance of simultaneously two hot spots (a-shot 138, left image) and a single hot spot (b-shot T140, right image).
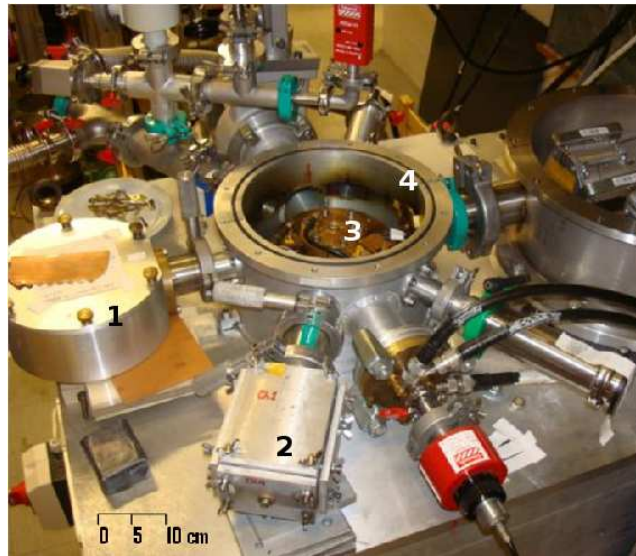
Figure 3. Photo of the experimental setup showing the arrangement of spectroscopic equipment. 1—de Broglie spectrometer with KAP crystal, 2—three crystal de Broglie spectrometer with pinhole, 3—compact de Broglie spectrometer, 4—discharge chamber.

4. Plasma source and spectroscopic equipment

Experiments were carried out at an X-pinch machine [26, 27] with a discharge current 220 kA. The voltage was 12 kV. In X-pinches the point-like plasma (or a hot spot) is formed in the vicinity of the cross point of the wires, so that the position of the plasma in radial and axial directions is more or less stable and reproducible. Plasma evolution varies too rapidly from mm to μm so that the measurements are usually integrated over space and time. Electron temperature and density are distributed in space and time with typical averaged values in the hot spot region of $T_e = 0.5$–1 keV, $n_e = 10^{25}$–10^{27} m^{-3} [28].

In our experiments Cu wires with diameter of 40 μ were used, the discharge axis (z) was vertical. Time integrated pinhole images (pinhole diameter 30 μ, covered by 20 μ Be.) are shown in figure 2. The distances from the plasma to the pinhole and the pinhole to the detector (BAS-TR 2025 image plate) were 200 mm and 100 mm, respectively. It was found that the hot plasma consists of 1–2 hot spots (see figure 2) with the typical hot spot sizes of 0.2–0.5 mm. The distance between the two hot spots was about 0.5 mm.

X-ray spectra were registered using 3 spectrometers:

(i) de Broglie type spectrometer, equipped with KAP crystal ($2d = 26.64$ Å, curvature radius $R = 250$ mm) designated as No^1 in figure 3. The KAP crystal was protected by Be a 15 μ filter and the dispersion plane was oriented perpendicular to the discharge axis (z). The distance between the plasma and the was 270 mm;

(ii) 3-mica crystals ($2d = 19.98$ Å) implemented in a spectrometer-polarimeter of de Broglie type [20], No^2 in figure 3. The curvature radius was 20 mm, the sizes of spectral slits were 1×13 mm^2, covered by 20μ Be foil. A pinhole (diameter 30μ) was mounted on the entrance window of the spectrometer. The dispersion planes of the channels were oriented in vertical and horizontal directions. The distance from the plasma to the crystal was 270 mm;

(iii) super compact ($43 \times 43 \times 25$ mm^3) de Broglie spectrometer-polarimeter (No^3 in figure 3), equipped by two mutually perpendicular mica crystals mounted in the channels #1 and #2 correspondingly. The curvature radius of crystals was 10 mm. The entrance slit of size 1×4 mm^2 have been protected by two layers of 6 μ mylar covered by 0.15 μ of Al.

The dispersion plane of ch#1 in figure 3 is vertical (parallel to the discharge axis Z), while that of ch#2 is horizontal. The small sizes of the mini spectrometer allowed us to mount them inside the discharge chamber so that distance from the plasma to crystal distance could be kept small: 65 mm only providing high luminosity and large spectral range.

The optical axis of the spectrometers was carefully aligned in order to intersect the same plasma region. The De Broglie spectrometers permitted to record large spectral range from 8.5–14 Å in a single shot. To record spectra and plasma images $Industrex$ x-ray film and $BAS-TR2025$ image plates (without protected layer) were used (being processed by FLA-7000 scanner).

Spectrometers ii-iii) served for polarization analysis according to the two crystal scheme shown in figure1. Since the L-shell lines of CuXX, $\lambda = 12.570$ Å and $\lambda = 12.8277$ Å are reflected at Bragg angles 38.98° and 39.94°, respectively, π- and σ- polarization components were selected with rather high purity (not less than 90%).

The reflectivity of KAP crystal is about 10 times higher than those of mica. Therefore, spectra taken with the KAP crystal spectrometer is very useful for registration and interpretation as spatial resolution could easily be realized while keeping a good signal to noise ratio: the entrance slit has a size of 0.14×5 mm^2. A photo from the experimental setup and the spectroscopic equipment is shown in figure 3 spectrometer equipped with a KAP crystal (No^1) is located on the left side, the spectrometer equipped with three mica crystals (No^2) is located in the center and the mini spectrometer (No^3) is located inside the discharge chamber (No^4).

5. Spectra of CuXX–CuXXI

Figure 4 shows the spectra in the range from (9.1–12.8) Å recorded with KAP in a single shot(black line). The most prominent lines belong to Ne-like copper (CuXX). Their spectroscopic notations and wavelengths are given in table 1. The wavelength scale in figure 5 is established from CuXX (Ne-like) and CuXXI (F-like) line spectra employing the identified emission lines #1–#9 from table 1 as reference lines (marked by green vertical lines in figure 4). The dispersion curve between the each pair of lines #1 – #9 is interpolated by eight cubic polynomials. The intensity ratio of the 3C line to its dielectronic Na-like satellites (transitions near 1.3 nm, see figure 4) may serve for electron temperature determination [19]. Likewise, the intensity ratio of the 3C line to the lines of F-like Cu XXI ions might be used to estimate the ionization temperature. For both ratios the dependence on electron density n_e is not very strong. On the other hand, the intensity ratios 3B/3C and 3G/3C of Ne-like CuXX resonance lines are strongly density dependent. At present, the theoretical model suppose that the respective lines in the line ratio methods are not polarized which could not be confirmed in the present experiments: line ratios are strongly dependent on the polarization.

Spectral lines, belonging to the transitions in F-like Cu marked F1, F2, F3 (transitions $2p^5 - 2p^4 3d$ and F4 ($2p^5 - 2p^4 3s$), have been also observed in the experiment. Their line center positions (taken from NIST), are shown in figure 4 with the blue vertical lines. As the positions of the line F1–F4 lines are well matched with those from NIST (blue lines) our interpolation procedure is shown to be very precise. The densitogram for shot T125 is taken along the central part of the spectrum (indicated by the white dotted rectangular inserted in the x-ray image of figure 4).

Spectra recorded by the channel of compact de Broglie spectrometer are shown in Figure 5 for the same shot T125 and the corresponding pinhole plasma image is presented in figure 6. Here, the plasma emission consists of two hot spots (#1 and #2) that are shifted in the

Table 1. Wavelengths of soft x-ray transitions in Ne-like copper CuXX.

| n°	transition	wavelength, Å	notation
1	$2s^2 2p^6\ ^1S_0 - 2s^2 2p^6 3p\ ^1P_1$	10.597	3A
2	$2s^2 2p^6\ ^1S_0 - 2s^2 2p^6 3p\ ^3P_1$	10.653	3B
3	$2s^2 2p^6\ ^1S_0 - 2s^2 2p^5 3d\ ^1P_1$	11.383	3C
4	$2s^2 2p^6\ ^1S_0 - 2s^2 2p^5 3d\ ^3D_1$	11.594	3D
5	$2s^2 2p^6\ ^1S_0 - 2s^2 2p^5 3d$	11.7360	3E
6	$2s^2 2p^6\ ^1S_0 - 2s^2 2p^5 3s\ ^1P_1$	12.570	3F
7	$2s^2 2p^6\ ^1S_0 - 2s^2 2p^5 3s\ ^3P_1$	12.8277	3G
8	$2s^2 2p^6\ ^1S_0 - 2s^2 2p^5 4d\ ^1P_1$	9.106	4A
9	$2s^2 2p^6\ ^1S_0 - 2s^2 2p^5 4d\ ^3D_1$	9.237	4B
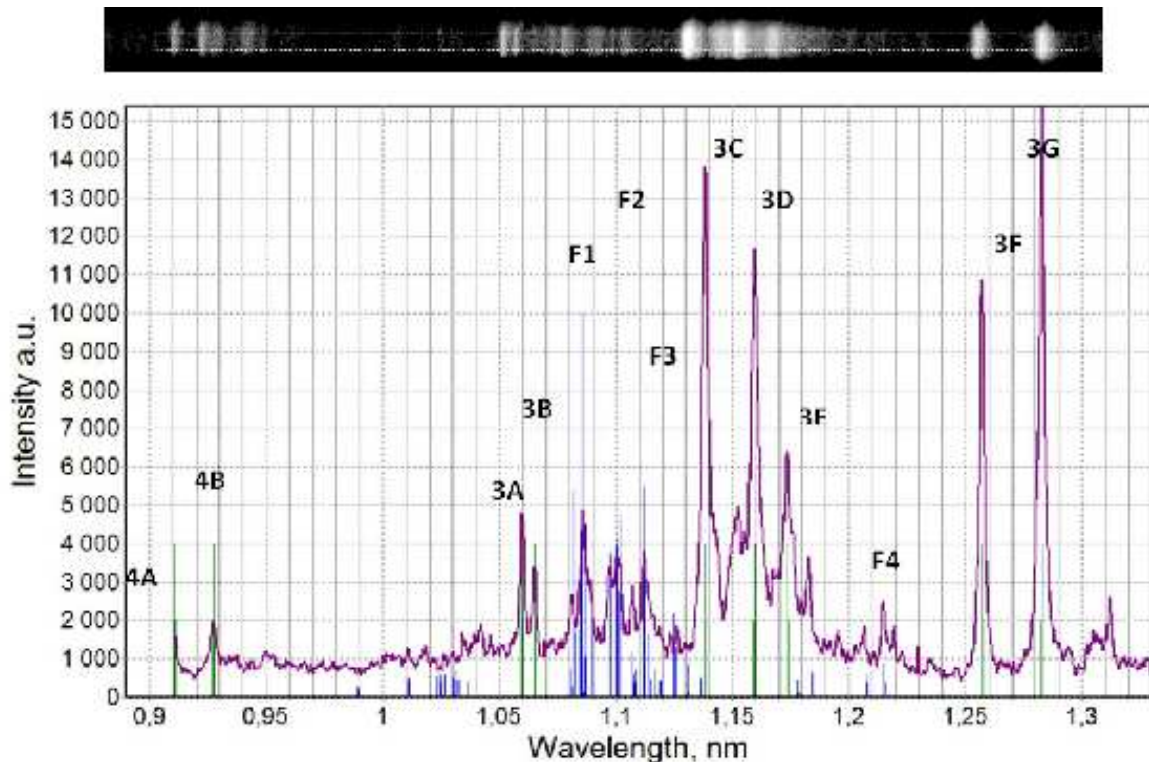
Figure 4. x-ray image and spectra from copper L-shell (shot T135) taken with de Broglie spectrometer equipped with a KAP crystal. Green and blue vertical lines indicate the reference lines, the violet curve is the experimental spectrum taking into account the transmission of the 15 μ thick Be filter.

vertical direction with respect to each other by about 0.5 mm. The spectrum on the left side of figure 5 (channel #1, vertical dispersion plane) shows the double structure: spectra, emitted by the hot spot #1 is shifted in wavelengths with respect to the spectra emitted by hot spot #2. The spectra on the right side of figure 5 (channel #2, dispersion plane is horizontal), does not demonstrate a double structure since both hot spots are on the same line of sight. Figure 5
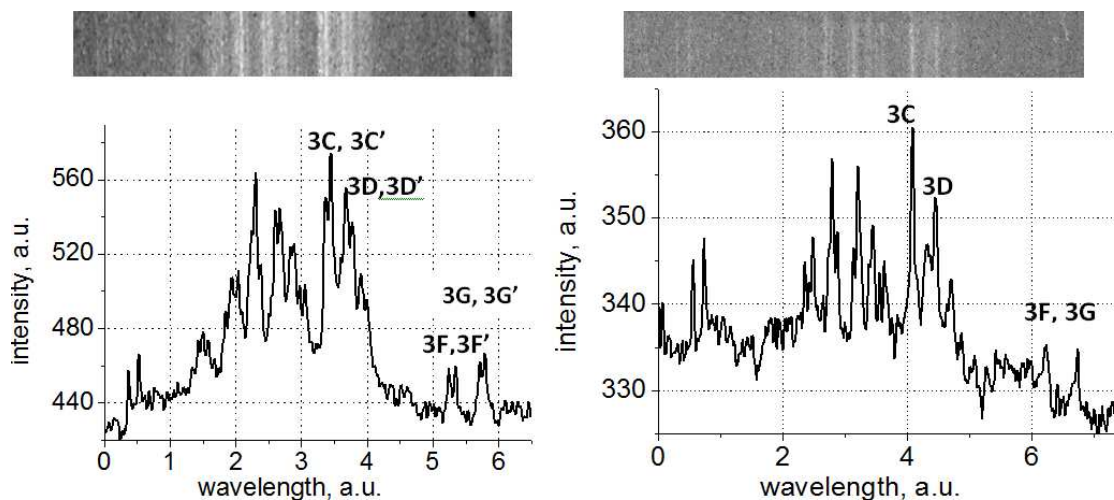
Figure 5. Double structure of CuXX–CuXXI spectra (on the left). Spectra are taken in the channel #1 (to the left, dispersive plane is vertical) and the channel #2 (to the right, dispersive plane is horizontal) of compact spectrometer, detector–film "Industrex", shot T125.
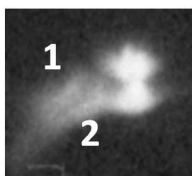
**Figure 6.** Double source in T125.
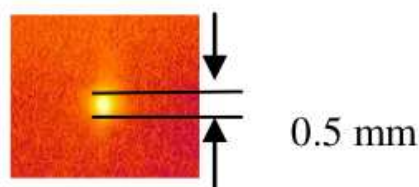
Figure 7. Pinhole image of shot T140 showing a single hot spot.

demonstrates that it is important to control the geometrical location of the hot spots: in order to perform polarization analysis one has to ensure that both spectrometers are recording the emission from the same hot spots.

6. Results of polarization analysis

In this section we present the results of polarization analysis concerning the Ne-like 3F and 3G lines that are quite isolated, see figure 4. According to the forgoing discussion, we have carefully selected spectra that result from a single hot spot only and do not show any asymmetric or double peaks line profiles as those discussed in relation with figure 5. We note that pinhole images are registered for each shot to control the plasma size and geometry of the hot spot. As discussed above, recorded spectra are space and time integrated.

The results of polarization measurements are carried out for the shot T140. The two multi-
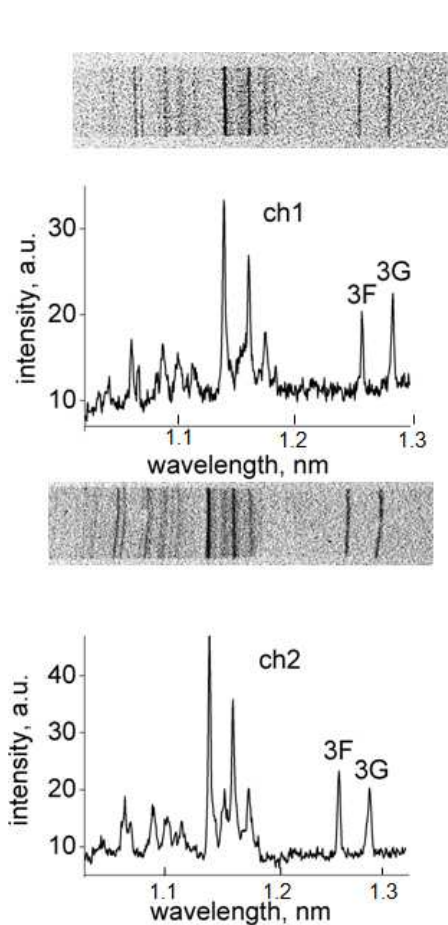
Figure 8. Spectra of Cu in the range 10.5–13 Å, registered in channels 1 and 2 of 3-crystal spectrometer. Shot T140.
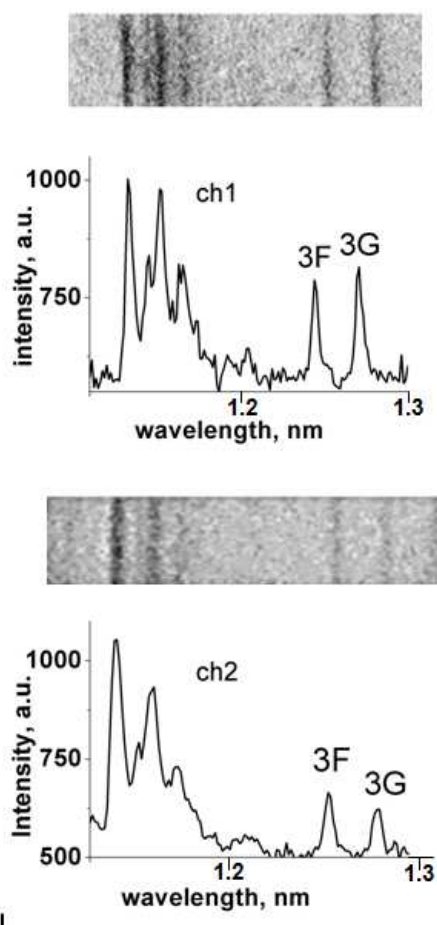
Figure 9. Spectra, taken in two channels of compact spectrometer–polarimeter, shot T140.

channel mica spectrometers ii) and iii) served as polarimeters. Figure 7 shows the plasma image obtained from the pinhole. Channels #1 of both polarimeters reflect the electric field vector perpendicular to the discharge axis z, while the electric field vector reflected in channels #2 was parallel to z. Spectra, from the 3-crystal spectrometer and corresponding densitogramms are shown in figure 8. The intensity of 3F line is less than that of 3G line in the channel #1 contrary to the channel #2 where intensity of 3F line exceeds that of 3G line. In figure 8 the intensity ratio 3C/3D/3E is the same for the channels #1&#2.

In order to considerably increase the confidence level of these observations we have recorded the same spectral range with the compact spectrometer-polarimeter, Figure 9. It can clearly be seen that spectra in channel #1 show a 3F line that is less intense compared to the 3G line, while the spectrum taken in channel #2 shows that the 3G line is more intense than the 3F line. We are therefore highly confident to have observed a polarization effect in Ne-like line ratios of copper CuXX.

We note that the phenomenon shown in figures 8 and 9 has been observed for many shots, so we are also confident that the result is reproducible and therefore a characteristic feature of the X-pinch. Due to the simultaneous observation of plasma emission by pinholes, we are likewise confident that only shots are analyzed that show a single hot spot.

Finally we note, that the crystal reflectivity changes by less than 1 per cent for the 3F and 3G CuXX lines because they are very close in energy (within 20 eV).

The 3F and 3G lines are reflected at Bragg angles 38.98° and 39.94°, respectively. According to the formula for crystal reflectivity the reflection for x-rays polarized perpendicular to the crystal is virtually zero: the spectrum contains only x-rays with their polarization parallel to the crystal. If the crystals are ideal mosaic the relative efficiency is $I_\sigma/I_\pi = \cos^2 2\theta = 0.04$, where I_σ and I_π are the intensities of the σ- and π-components, respectively. Thus, for the mica crystal the effectiveness of the separation of the σ- and π-components $(I_\sigma - I_\pi)/(I_\sigma + I_\pi)$ is 92%. In this respect we mention that the KAP crystal does not well separate the polarized components for the 3F and 3G lines, because $I_\sigma/I_\pi = cos^2 2\theta = 0.3$. Therefore the effectiveness of the separation of $(I_\sigma - I_\pi)/(I_\sigma + I_\pi)$ is only 54%.

We have also analyzed in which manner the convex geometry of the bend crystals might affect the line intensities. In our experiments, the radial and axial displacement of the hot spot from shot to shot is about 0.3–0.5 mm. This is obviously within the field of view for both channels of both spectrometers. For a point-like source only a small part of the crystal reflects the line and therefore the line intensity depends on the local reflection coefficient of the crystal [29]. For the presently employed geometry, the crystal zones that reflect the 3F&3G lines are overlapping, the distance between their centers are less than 0.25 mm while their length is about 0.5 mm. At the same time, the local zones reflecting the 3F & 3G lines are shifted along the crystal surface from shot to shot due to slightly different locations of the hot spots. However, as we have observed many single shot spectra we observe that the different in the line intensity ratios 3F/3G for both spectrometers and both channels remained the same. We therefore can exclude local crystal defects and spatial hot spot variation to have influenced the present observations of figures 8 and 9.

Having confirmed the polarization dependence of the 3F and 3G lines we can conclude that the evaluation of plasma parameters that is based on line ratios has to be taken into account selective excitation of m-components whereas neglecting of polarization effects might result in questionable parameter determinations. Despite of many publications on polarized radiation from plasmas over the last decades [10], most of the commonly available codes do not include polarization effects. It remains there a challenge to quantitatively interpret x-ray polarization measurements to characterize anisotropic energetic electrons [9] and the strong electric and/or magnetic fields [27].

7. Summary

We have performed x-ray polarization spectroscopy of CuXX L-shell line spectra emitted from a high current X-pinch with an exceptional confidence level employing simultaneously two polarization spectrometers each equipped with two Bragg mica crystals. Time integrated spectra from single shots have been preselected for single hot spot emission only with the help of pinhole images. In addition survey spectra have been obtained with a spectrometer equipped with a curved KAP Bragg crystalI covering the large spectral range from about 1.0 nm until 1.3 nm to observe L-shell line emission from higher charge states. The pair of spectrally well resolved Ne-like resonance lines originating from the singlet and triplet 3s-sates $1s^2 2s^2 2p^5 3s\ ^1P_1$ and $1s^2 2s^2 2p^5 3s\ ^3P_1$ show clear evidence of line polarization. Due to the high quality of the data combined with the high confidence level achieved in the polarization measurements the obtained high-resolution x-ray spectra may serve as a unique input for future detailed theoretical analysis.

Acknowledgments

References

[1] Vikhrev V V, Dobriakov A V and Rosanova G A 1989 *Plasma Phys. Rep.* **15** 584
[2] Koshelev K N and Pereira N R 1990 *J. Appl. Phys.* **69** R21
[3] Gordeev A V and Loseva T V 2003 *Plasma Phys. Rep.* **29**809
[4] Vikhrev V V and Braginski S I 1986 *Rev. Plasma Phys.* **10**
[5] Liberman M A, De Groot J S, Toor A 1998 *Physics of High Density Plasma Springler*
[6] Vinogradov A V 1975 *Kvant. Elektron.* **2** 1165
[7] Aglickiy E V, Boiko V A and Pikuz S A 1974 *Kvant. Elektron.* **1** 579
[8] Faucher P, Peyraud-Cuenca N and Rosmej F B 2010 *J. Plasma Phys.* **100** l63 3 255
[9] Inal M K and Dubau J 1987*J. Phys. B: At. Mol. Phys.* **20** 4221
[10] Rosmej F B 2012 *Highly Charged Ion Spectroscopic Research* ed. Y Zou and R Hutton (Taylor and Francis 267-341 ISBN: 978-1-4200-7904-3)
[11] Fujimoto T and Iwamae A (eds) 2007 *Plasma Polarization Spectroscopy* (Springer) p 154
[12] Korchak A A 1967 *Dokl. Akad. Nauk SSSR* **172** 306
[13] Inubushi Y, Kai T, Nakamura T, Fujioka S, Nishimura H and Mima K 2007 *Phys. Rev.* E **75** 026401
[14] Veretennikov V V, Gurei A N *et al*1989 *Plasma Phys. Rep.* **7** 1199
[15] Baronova E O, Sholin G V and Jakubowski L 1999 *JETP Lett.* **69** 25
[16] Jakubowski L, Sadowski M and Baronova E 2004 *Chech. J. Plasma Phys.* 54 Suppl C SPPT271 1 C1–C6
[17] Jakubowski L, Sadowski M and Baronova E 2004 *Nucl. Fusion* **44** 1
[18] Beiersdorfer P, Vogel D A, Reed K J, Decaux V, Scofield J H, Widmann K, Hölzer G, Förster E, Wehrhan O and Savin D W 1996 *Phys. Rev.* A **53** 3974
[19] Shelkovenko T A, Skobelev I Y, Pikuz S A and Etlisher A B 1996 *Kvant. Elektron.* **23** 137
[20] Baronova E O, Bucher D, Haas D, Fedin D, Stepanenko A and Beg F 2006 *Rev. Sci. Instrum.* **77** 1
[21] Percival I C and Seaton M J 1958 *Phil. Trans. R. Soc. London* **1251** 113
[22] Fujimoto T and Iwamae A (eds) 2008 *Springer Berlin ISBN 978-3-540-735861*
[23] Vinogradov A V, Urnov A M and Shlyaptseva A S 1989 *Proceedings of the Lebedev Physics Institute of Russian Academy of Sciences* **192** 93
[24] Baronova E O, Stepanenko M M, Sholin G V, Vikhrev V V, Jakubowski L and Fujimoto T 2004 *Proc of Polarization Spectroscopy Workshop Kyoto*
[25] Sholin G V 1967 *Dokl. Akad. Nauk SSSR* **175** 256
[26] Larour J, Aranchouk L E and Chuvatin A S 2005 *IEEE Trans. Plasma Sci.* **33**
[27] Larour J and Aranchouk L E 2006 *J. de Physique IV France* **138**
[28] Chgandler K M, Quart N D, Hansen S B, Mitchel M D, Pikuz S A, Shelkovenko T A, Hammer D A, Kantsyrev V L and Fedin D A 2010 *Rev. Sci. Instr.* **75** 3702
[29] Lider V V, Baronova E O and Stepanenko M M 2001 *Crystallogr. Rep.* **46** 341